文章编号:1674-2974(2024)11-0187-10 DOI:10.16339/j.cnki.hdxbzkb.2024120

# 水平瞬态荷载作用下桩土动力相互作用研究

余云燕[1],冯一帆[1],王立安[2†]
(1. 兰州交通大学 土木工程学院,甘肃 兰州 730070;
2. 兰州交通大学 铁道技术学院,甘肃 兰州 730070)

**摘 要**:为研究桩基在桩-土界面连续条件下,桩顶受撞击等水平瞬态荷载作用时桩基位移响应、桩-土界面动力响应和桩周土的应力分布规律,根据Biot理论和Novak平面应变假定,采用Euler梁建立桩-饱和土耦合振动的平面应变简化模型,利用Laplace变换和势函数分解求解系统动力控制方程.针对桩-土系统在水平三角形冲击荷载作用下的振动状态,着重对桩基位移响应、桩-土界面和桩周土的动力响应开展时域分析.研究发现:桩-土系统的位移场响应滞后于应力场响应;桩土模量比越小,桩-土界面有效径向应力、切应力及孔压响应越显著;土体渗透系数减小引起桩-土界面孔压增大,导致有效径向应力减小,桩-土界面处切应力几乎不受渗透系数变化的影响;渗透系数较大时,桩周土孔压分布较分散,最大有效径向应力出现在桩-土界面附近;渗透系数较小时,桩周土孔压分布较为集中,最大有效径向应力则出现在桩-土界面较远处.

**关键词**:桩-土动力相互作用;饱和土;Novak平面应变假定;三角形冲击荷载;时域分析
**中图分类号**:TU473; **文献标志码**:A

# Study of Pile-soil Dynamic Interaction under Horizontal Transient Loads

YU Yunyan[1], FENG Yifan[1], WANG Li'an[2†]
(1. School of Civil Engineering, Lanzhou Jiaotong University, Lanzhou 730070, China;
2. Institute of Railway Technology, Lanzhou Jiaotong University, Lanzhou 730070, China)

**Abstract**: To study the displacement response of pile foundations, the dynamic response of pile-soil interface, and the law of stress distribution in the soil around the pile when the top of the pile is subjected to horizontal transient loads, such as impact, under the condition of continuity of the pile-soil interface, the simplified model of pile-saturated soil coupling vibration is established using the Euler beam based on the Biot theory and Novak plane strain assumption. The system's dynamic control equations are solved using Laplace transformation and potential function decomposition. The focus is on the time-domain analysis of the vibration response of the pile-soil system under horizontal triangular impact loading, including pile displacement response, pile-soil interface, and dynamic response of the soil around the pile. The research reveals that the displacement field response of the pile-soil system lags behind the stress field response. Moreover, as the pile-soil modulus ratio decreases, the effective radial stress,

* **收稿日期**:2023-12-05
**基金项目**:甘肃省科技计划资助项目(23JRRA854,22JR11RA155),Science and Technology Program of Gansu Province(23JRRA854,22JR11RA155)
**作者简介**:余云燕(1968—),女,浙江江山人,兰州交通大学教授,博士
† 通信联系人,E-mail: 513173705@qq.com

shear stress, and pore pressure responses at the pile-soil interface become more pronounced. A decrease in soil permeability coefficient leads to increasing pore pressure at the pile-soil interface, causing a reduction of effective radial stress. The shear stress at the pile-soil interface remains almost unchanged with varying permeability coefficients. For higher permeability coefficients, the pore pressure distribution around the pile is more dispersed, and the maximum effective radial stress occurs near the pile-soil interface. Conversely, for lower permeability coefficients, the pore pressure distribution around the pile is more concentrated, and the maximum effective radial stress occurs at a greater distance from the pile-soil interface.

**Key words**: pile-soil dynamic interaction; saturated soil; Novak plane strain assumption; triangular impact load; time-domain analysis

桩基础因其抗震性能佳、沉降量小及能解决特殊地基承载力问题,常用于动力机械基础、交通设施和海洋工程.在这些应用中,桩基础可能遭受动力机械启动的瞬时振动、车辆碰撞、船舶撞击等冲击荷载,由于冲击荷载的突发性和瞬时性,其作用机理相较于静载和简谐荷载更加难以预测.

关于桩-土动力接触问题,国内外学者已进行广泛研究,除了以有限元、边界元为代表的数值方法外,还有以动力Winkler地基梁模型和连续介质模型为主的解析和半解析方法.动力Winkler地基梁模型采用并联弹簧和黏壶近似代替桩周土体的刚度和阻尼,考虑土体随荷载和深度的非线性变化,因其物理概念清晰、计算简单,成为分析桩-土相互作用的有效手段.Nogami等[1-2]基于该模型,率先分析了弹性桩在轴向冲击荷载下的瞬态响应.此后大部分学者沿用此法,将桩周土简化为Winkler地基来研究单桩瞬态响应.然而,Winkler地基模型在真实反映桩-土相互作用方面存在局限,土体刚度和阻尼系数合理取值存在困难,且无法考虑应力波在土层中的传播效应.

连续介质模型将土体视为连续体,Novak等[3-6]将桩周土考虑为相互独立的薄土层,建立了经典的平面应变模型,在此基础上研究了单桩振动特性.Gazetas等[7]基于平面应变模型和分象限假设,推导了单相介质中桩的辐射阻尼表达式.尚守平等[8]将Novak平面应变模型从单相土拓展至饱和土中,研究了饱和土中端承桩水平振动特性,分析了桩土模量比、渗透系数等对桩顶复阻抗的影响.余俊等[9-11]研究了饱和土的渗透系数对Biot动力方程的影响,并讨论了桩-土相互作用体系中不同简化假定的适用性.刘林超等[12]进一步研究了饱和土中管桩和群桩的水平振动.Hu等[13]、赵密等[14]针对海上风机,研究了部分埋入式桩基的水平振动.范小雪等[15]基于平面应变假定,探讨了饱和土中缺陷桩水平振动,验证了平面应变简化模型在饱和土中桩水平动力响应研究中的适用性.郑长杰等[16-17]则考虑饱和桩周土和桩芯土,研究了管桩振动特性.Hu等[18]考虑了土体的径向非均质性,研究了饱和土中端承桩在不同荷载组合形式下的水平动力响应问题.Zheng等[19]基于三维连续介质,研究了大直径管桩的水平振动.章敏等[20]和郭诚[21]系统研究了非饱和土中端承桩和管桩的水平振动特性.杨紫健等[22]研究了有竖向荷载影响的非饱和地基中桩的水平振动.Mamoon等[23]研究了水平冲击荷载下单相弹性地基中桩基的时域响应.刘圆圆等[24]将平面应变模型应用于桩水平振动时域响应分析,考察了桩土模量比、渗透系数、长径比对桩顶位移和桩身弯矩的影响.尚微[25]基于连续介质模型,研究了管桩水平冲击荷载下的桩顶位移响应,分析了冲击形式、时间和桩径对桩顶位移的影响,以及桩土模量比对桩身变形和内力的影响.赵仓龙等[26]研究了层状饱和土中管桩的瞬态扭转振动.

由文献[1-27]可知,桩-土水平相互作用的研究多聚焦于频域分析,时域研究相对较少.现有时域研究主要探讨桩基位移、内力、动阻抗与桩身尺寸、桩土模量比、渗透系数的关系,却忽视了振动状态下桩-土界面以及桩周土的力学行为.

基于此,本文针对水平冲击荷载下的桩-土系统的振动状态,着重对桩基位移响应、桩-土界面和桩周饱和土的动力响应开展时域分析.首先,采用Biot饱和多孔介质来描述饱和土层,构建严格桩-成层饱

和土水平耦合振动的平面应变简化模型.然后,通过Laplace变换、势函数分解及分离变量法求解桩-土系统的动力控制方程,得出Laplace变换域的桩身位移和桩周饱和土应力表达式.最后,利用Laplace逆变换计算三角形冲击荷载下桩-土系统的时域响应,进行参数分析.

## 1　分析模型与基本假定

### 1.1　分析模型

如图1所示,采用三维柱坐标系构建桩-土耦合振动计算模型,$r$为径向坐标,$\theta$为切向坐标(逆时针为正),$z$为沿桩身纵向坐标.$H$为桩长,$r_0$为半径,桩底自由.

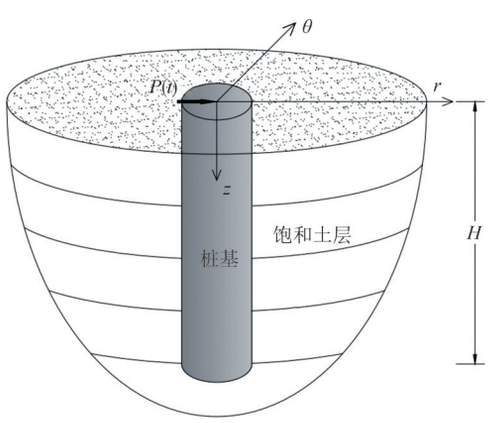



图1　桩-土系统计算模型

Fig.1　Pile-soil system calculation model

对于桩顶冲击荷载形式的选择,三角形冲击荷载相较于正弦冲击荷载、矩形冲击荷载等具有短时间内达到峰值后迅速减小为零的特点.因此,本文采用三角形冲击荷载来准确模拟桩基受到的短暂冲击动荷载.三角形冲击荷载$P(t)$表达式为:

$$P(t)=2P_{\max}\frac{t}{t_0}f_{\mathrm{H}}\left(\frac{t_0}{2}-t\right)+2P_{\max}\left(1-\frac{t}{t_0}\right)\left[f_{\mathrm{H}}\left(t-\frac{t_0}{2}\right)-f_{\mathrm{H}}(t-t_0)\right] \tag{1}$$

式中:$P_{\max}$为荷载峰值,$t_0$为荷载作用时长,$f_{\mathrm{H}}(\cdot)$为Heaviside阶跃函数.式(1)中引入时间因子$t$的Laplace变换,得到三角形冲击荷载在Laplace变换域中的表达式为:

$$\tilde{P}(s)=\frac{2P_{\max}}{t_0 s^2}\left(1-\mathrm{e}^{-t_0 s/2}\right)^2 \tag{2}$$

式中:$\tilde{P}(s)$是$P(t)$的Laplace变换式,$s$为变换参数.

### 1.2　基本假定

1)桩周土体由两相饱和薄土层组成,薄土层之间相互独立且沿纵向忽略竖向连续.

2)桩-土系统水平振动时,桩侧薄土层之间保持充分接触,忽略土体竖向位移和桩侧摩阻力.

3)桩基为弹性圆柱体,垂直于半空间表面,采用Euler梁模型.

4)桩-土系统水平振动过程为小变形,桩-土界面不发生分离为完全接触,且桩-土接触面不透水.

## 2　控制方程

### 2.1　饱和土控制方程

针对桩-饱和土水平振动,采用Biot饱和多孔介质理论,忽略土体竖向位移,建立桩周饱和土控制方程:

$$\mu\nabla^2 u_{\mathrm{r}}+(\lambda_{\mathrm{c}}+\mu)\frac{\partial e}{\partial r}-\frac{\mu}{r^2}\left(2\frac{\partial u_\theta}{\partial\theta}+u_{\mathrm{r}}\right)-\alpha M\frac{\partial\varepsilon}{\partial r}=\rho\ddot{u}_{\mathrm{r}}+\rho_{\mathrm{f}}\ddot{w}_{\mathrm{r}} \tag{3}$$

$$\mu\nabla^2 u_\theta+(\lambda_{\mathrm{c}}+\mu)\frac{1}{r}\frac{\partial e}{\partial\theta}-\frac{\mu}{r^2}\left(u_\theta-2\frac{\partial u_{\mathrm{r}}}{\partial\theta}\right)-\alpha M\frac{1}{r}\frac{\partial\varepsilon}{\partial\theta}=\rho\ddot{u}_\theta+\rho_{\mathrm{f}}\ddot{w}_\theta \tag{4}$$

$$\alpha M\frac{\partial e}{\partial r}-M\frac{\partial\varepsilon}{\partial r}=\rho_{\mathrm{f}}\ddot{u}_{\mathrm{r}}+m\ddot{w}_{\mathrm{r}}+b\dot{w}_{\mathrm{r}} \tag{5}$$

$$\alpha M\frac{1}{r}\frac{\partial e}{\partial\theta}-M\frac{1}{r}\frac{\partial\varepsilon}{\partial\theta}=\rho_{\mathrm{f}}\ddot{u}_\theta+m\ddot{w}_\theta+b\dot{w}_\theta \tag{6}$$

式中:$u_{\mathrm{r}}$、$w_{\mathrm{r}}$分别为土骨架和水相对于土骨架的径向位移;$u_\theta$、$w_\theta$分别为土骨架和水相对于土骨架的切向位移;$\lambda$、$\mu$为Lamé常数;$e$、$\varepsilon$分别为土骨架和水的体应变;$\alpha$、$M$分别为反映土颗粒和水压缩性的Biot系数,$\lambda_{\mathrm{c}}=\lambda+\alpha^2 M$,$m=\rho_{\mathrm{f}}/n$,$b=\rho_{\mathrm{f}}g/k_{\mathrm{d}}$;$\rho$为土体总密度,$\rho=\rho_{\mathrm{s}}(1-n)+n\rho_{\mathrm{f}}$;$\rho_{\mathrm{s}}$、$\rho_{\mathrm{f}}$分别为固体颗粒和水的密度;$k_{\mathrm{d}}$为渗透系数;$g$为重力加速度;$n$为孔隙率;$\nabla^2$为Laplace算子.

### 2.2　桩基控制方程

采用Euler梁模型建立桩基控制方程:

$$\pi {r_0}^2\rho_{\mathrm{p}}\frac{\partial^2 u_{\mathrm{p}}}{\partial t^2}+E_{\mathrm{p}}I_{\mathrm{p}}\frac{\partial^4 u_{\mathrm{p}}}{\partial z^4}+q_{\mathrm{n}}=0 \tag{7}$$

式中:$u_{\mathrm{p}}$为桩基水平位移;$E_{\mathrm{p}}$、$I_{\mathrm{p}}$、$r_0$、$\rho_{\mathrm{p}}$、$q_{\mathrm{n}}$分别为桩基弹性模量、截面惯性矩、截面半径、密度和桩-土相互作用的荷载集度.

### 2.3 定解条件

桩-土系统初始条件为:

$$u_{\mathrm{p}}、u_{\mathrm{r}}、u_{\theta}\big|_{t=0}=0 \tag{8}$$

$$\sigma_{\mathrm{r}}'、\tau_{\mathrm{r}\theta}、P\big|_{t=0}=0 \tag{9}$$

土体在径向无穷远处边界条件为:

$$u_{\mathrm{r}}、u_{\theta}\big|_{r=\infty}=0 \tag{10}$$

$$\sigma_{\mathrm{r}}'、\tau_{\mathrm{r}\theta}、P\big|_{r=\infty}=0 \tag{11}$$

考虑桩土完全接触,则桩-土界面边界条件为:

$$u_{\mathrm{r}}\big|_{r=r_0}=u_{\mathrm{p}}\cos\theta,\ u_{\theta}\big|_{r=r_0}=-u_{\mathrm{p}}\sin\theta \tag{12}$$

桩-土界面不透水条件为:

$$w_{\mathrm{r}}|_{r=r_0}=0 \tag{13}$$

桩顶边界条件为:

$$E_{\mathrm{p}}I_{\mathrm{p}}\partial^2u/\partial z^2\big|_{z=0}=0,\ E_{\mathrm{p}}I_{\mathrm{p}}\partial^3u/\partial z^3\big|_{z=0}=P(t) \tag{14}$$

水平荷载作用于桩顶通常对桩身上部影响显著,对桩身下部影响很小,所以桩底采用自由支撑边界条件:

$$\partial^2u/\partial z^2\big|_{z=H}=0,\ \partial^3u/\partial z^3\big|_{z=H}=0 \tag{15}$$

## 3 方程求解

### 3.1 饱和土控制方程求解

采用Helmholtz分解$u_{\mathrm{r}}、w_{\mathrm{r}}$:

$$\begin{cases}u_{\mathrm{r}}=\dfrac{\partial\varphi_{\mathrm{s}}}{\partial r}+\dfrac{1}{r}\dfrac{\partial\phi_{\mathrm{s}}}{\partial\theta},\ u_{\theta}=\dfrac{1}{r}\dfrac{\partial\varphi_{\mathrm{s}}}{\partial\theta}-\dfrac{\partial\phi_{\mathrm{s}}}{\partial r}\\ w_{\mathrm{r}}=\dfrac{\partial\varphi_{\mathrm{f}}}{\partial r}+\dfrac{1}{r}\dfrac{\partial\phi_{\mathrm{f}}}{\partial\theta},\ w_{\theta}=\dfrac{1}{r}\dfrac{\partial\varphi_{\mathrm{f}}}{\partial\theta}-\dfrac{\partial\phi_{\mathrm{f}}}{\partial r}\end{cases} \tag{16}$$

式中:$\varphi_{\mathrm{s}}、\phi_{\mathrm{s}}、\varphi_{\mathrm{f}}、\phi_{\mathrm{f}}$均为势函数.

将式(16)分别代入式(3)~式(6),对时间域进行Laplace变换,变换公式为$\tilde{f}(r,s)=\int_0^{+\infty}f(r,t)\mathrm{e}^{-st}\mathrm{d}t$,可得:

$$\begin{cases}(\lambda_{\mathrm{c}}+2\mu)\nabla^2\tilde{\varphi}_{\mathrm{s}}+\alpha M\nabla^2\tilde{\varphi}_{\mathrm{f}}-\rho s^2\tilde{\varphi}_{\mathrm{s}}-\rho_{\mathrm{f}}s^2\tilde{\varphi}_{\mathrm{f}}=0\\ \mu\nabla^2\tilde{\phi}_{\mathrm{s}}-\rho s^2\tilde{\phi}_{\mathrm{s}}-\rho_{\mathrm{f}}s^2\tilde{\phi}_{\mathrm{f}}=0\\ \alpha M\nabla^2\tilde{\varphi}_{\mathrm{s}}+M\nabla^2\tilde{\varphi}_{\mathrm{f}}-\rho_{\mathrm{f}}s^2\tilde{\varphi}_{\mathrm{s}}-ms^2\tilde{\varphi}_{\mathrm{f}}-bs\tilde{\varphi}_{\mathrm{f}}=0\\ \rho_{\mathrm{f}}s^2\tilde{\phi}_{\mathrm{s}}+ms^2\tilde{\phi}_{\mathrm{f}}+bs\tilde{\phi}_{\mathrm{f}}=0\end{cases} \tag{17}$$

式中:$\tilde{\varphi}_{\mathrm{s}}、\tilde{\varphi}_{\mathrm{f}}、\tilde{\phi}_{\mathrm{s}}、\tilde{\phi}_{\mathrm{f}}$分别为$\varphi_{\mathrm{s}}、\varphi_{\mathrm{f}}、\phi_{\mathrm{s}}、\phi_{\mathrm{f}}$的拉式变换,$s$为时间因子$t$的拉式变换.

将上式写成矩阵形式:

$$\begin{bmatrix}(\lambda_{\mathrm{c}}+2\mu)\nabla^2-\rho s^2 & \alpha M\nabla^2-\rho_{\mathrm{f}}s^2\\ \alpha M\nabla^2-\rho_{\mathrm{f}}s^2 & M\nabla^2-ms^2-bs\end{bmatrix}\begin{bmatrix}\tilde{\varphi}_{\mathrm{s}}\\ \tilde{\varphi}_{\mathrm{f}}\end{bmatrix}=0 \tag{18}$$

$$\begin{bmatrix}\mu\nabla^2-\rho s^2 & -\rho_{\mathrm{f}}s^2\\ \rho_{\mathrm{f}}s^2 & ms^2+bs\end{bmatrix}\begin{bmatrix}\tilde{\phi}_{\mathrm{s}}\\ \tilde{\phi}_{\mathrm{f}}\end{bmatrix}=0 \tag{19}$$

式(18)为微分算子方程,要使$\tilde{\varphi}_{\mathrm{s}}、\tilde{\varphi}_{\mathrm{f}}、\tilde{\phi}_{\mathrm{s}}、\tilde{\phi}_{\mathrm{f}}$有非平凡解,必须使微分算子行列式为零,则有:

$$\left(\nabla^4-d_1\nabla^2+d_2\right)\tilde{\varphi}_{\mathrm{s}}=0 \tag{20}$$

$$\left(\nabla^4-d_1\nabla^2+d_2\right)\tilde{\varphi}_{\mathrm{f}}=0 \tag{21}$$

式中:$d_1=\dfrac{\left(\lambda_{\mathrm{c}}+2\mu\right)\left(ms^2+bs\right)+M\rho s^2-2\alpha M\rho_{\mathrm{f}}s^2}{(\lambda+2\mu)M}$,

$d_2=\dfrac{\left(m\rho-\rho_{\mathrm{f}}{}^2\right)s^4+\rho bs^3}{(\lambda+2\mu)M}$.

由算子分解理论可知,$\tilde{\varphi}_{\mathrm{s}}=\tilde{\varphi}_{\mathrm{s1}}+\tilde{\varphi}_{\mathrm{s2}}$,且$\tilde{\varphi}_{\mathrm{s1}}、\tilde{\varphi}_{\mathrm{s2}}$满足:

$$(\nabla^2-\beta_1{}^2)\tilde{\varphi}_{\mathrm{s1}}=0 \tag{22}$$

$$(\nabla^2-\beta_2{}^2)\tilde{\varphi}_{\mathrm{s2}}=0 \tag{23}$$

式中:$\beta_1{}^2=\dfrac{d_1+\sqrt{d_1{}^2-4d_2}}{2}$,$\beta_2{}^2=\dfrac{d_1-\sqrt{d_1{}^2-4d_2}}{2}$.

再分离变量,令$\tilde{\varphi}_{\mathrm{s1}}=R_1(r)\Phi_1(\theta)$带入式(22)可得:

$$\Phi_1(\theta)\frac{\partial^2R_1(r)}{\partial r^2}+\Phi_1(\theta)\frac{1}{r}\frac{\partial R_1(r)}{\partial r}+R_1(r)\frac{1}{r^2}\frac{\partial^2\Phi_1(\theta)}{\partial\theta^2}-\beta_1{}^2R_1(r)\Phi_1(\theta)=0 \tag{24}$$

对式(24)求解可得:

$$\tilde{\varphi}_{\mathrm{s1}}=\left[A_{11}\sin\left(n_1\theta\right)+B_{11}\cos\left(n_1\theta\right)\right]\times\left[C_{11}K_{n_1}\left(\beta_1r\right)+D_{11}I_{n_1}\left(\beta_1r\right)\right] \tag{25}$$

同理可得:

$$\tilde{\varphi}_{\mathrm{s2}}=\left[A_{12}\sin\left(n_2\theta\right)+B_{12}\cos\left(n_2\theta\right)\right]\times\left[C_{12}K_{n_2}\left(\beta_2r\right)+D_{12}I_{n_2}\left(\beta_2r\right)\right] \tag{26}$$

式中:$I_{n_1}\left(\beta_1r\right)、K_{n_1}\left(\beta_1r\right)、I_{n_2}\left(\beta_2r\right)、K_{n_2}\left(\beta_2r\right)$分别为第一类和第二类修正Bessel函数;$A_{11}、A_{12}、B_{11}、B_{12}、C_{11}、C_{12}、D_{11}、D_{12}$和$n_1、n_2$均为待定系数.由边界条件式(10)、式(11)结合修正Bessel函数性质,可得:$D_{11}=D_{12}=0$;由$u_{\mathrm{r}}$为$\theta$的偶函数,$u_{\theta}$为$\theta$的奇函数,可得:$A_{11}=A_{12}=0$且$n_1=n_2=1$.

则有:

$$\tilde{\varphi}_{\mathrm{s}}=\left[A_1K_1\left(\beta_1r\right)+A_2K_1\left(\beta_2r\right)\right]\cos\theta \tag{27}$$

同理可得:

$$\tilde{\varphi}_{\mathrm{f}}=\left[A_4K_1\left(\beta_1r\right)+A_5K_1\left(\beta_2r\right)\right]\cos\theta \tag{28}$$

$$\tilde{\phi}_{\mathrm{s}}=\left[A_3K_1\left(\beta_3r\right)\right]\sin\theta \tag{29}$$

$$\tilde{\phi}_{\mathrm{f}}=\left[A_6K_1\left(\beta_3r\right)\right]\sin\theta \tag{30}$$

由$\tilde{\varphi}_s$、$\tilde{\varphi}_f$、$\tilde{\phi}_s$、$\tilde{\phi}_f$之间的相关性可得:

$$A_4 = a_1A_1, A_5 = a_2A_2, A_6 = a_3A_3 \tag{31}$$

式中:$A_1$~$A_6$为待定系数;$\beta_3{}^2 = \dfrac{\rho m s^4 + b\rho s^3 - \rho_f{}^2 s^4}{\mu\left(ms^2 + bs\right)}$,

$a_1 = \dfrac{\left(\lambda_c + 2\mu\right)\beta_1{}^2 - \rho s^2}{\rho_f s^2 - \alpha M\beta_1{}^2}$,　$a_2 = \dfrac{\left(\lambda_c + 2\mu\right)\beta_1{}^2 - \rho s^2}{\rho_f s^2 - \alpha M\beta_1{}^2}$,

$a_3 = -\dfrac{\rho_f s^2}{ms^2 + bs}$.

将式(27)~式(31)代入式(16),结合定解条件式(12)、式(13),可求得Laplace变换域中桩侧饱和土位移表达式:

$$\begin{cases} u_r = \left[A_1\dfrac{\partial K_1(\beta_1 r)}{\partial r} + A_2\dfrac{\partial K_1(\beta_2 r)}{\partial r} + \dfrac{A_3}{r}K_1(\beta_2 r)\right]\cos\theta \\ u_\theta = \left[-\dfrac{A_1}{r}K_1(\beta_1 r) - \dfrac{A_2}{r}K_1(\beta_2 r) - A_3\dfrac{\partial K_1(\beta_3 r)}{\partial r}\right]\sin\theta \end{cases} \tag{32}$$

$$\begin{cases} w_r = \left[a_1A_1\dfrac{\partial K_1(\beta_1 r)}{\partial r} + a_2A_2\dfrac{\partial K_1(\beta_2 r)}{\partial r} + \dfrac{a_3A_3}{r}K_1(\beta_2 r)\right]\cos\theta \\ w_\theta = \left[-\dfrac{a_1A_1}{r}K_1(\beta_1 r) - \dfrac{a_2A_2}{r}K_1(\beta_2 r) - a_3A_3\dfrac{\partial K_1(\beta_3 r)}{\partial r}\right]\sin\theta \end{cases} \tag{33}$$

式中:

$A_1 = \dfrac{\left[a_2b_2\left(b_3 + c_3\right) - a_3b_3\left(b_2 + c_2\right)\right]\tilde{u}_p}{a_1b_1\left(b_2c_3 - b_3c_2\right) - a_2b_2\left(b_1c_3 - b_3c_1\right) + a_3b_3\left(b_1c_2 - b_2c_1\right)}$,

$A_2 = \dfrac{\left[a_3b_3\left(b_1 + c_1\right) - a_1b_1\left(b_3 + c_3\right)\right]\tilde{u}_p}{a_1b_1\left(b_2c_3 - b_3c_2\right) - a_2b_2\left(b_1c_3 - b_3c_1\right) + a_3b_3\left(b_1c_2 - b_2c_1\right)}$,

$A_3 = \dfrac{\left[a_2b_2\left(b_1 + c_1\right) - a_1b_1\left(b_2 + c_2\right)\right]\tilde{u}_p}{a_1b_1\left(b_2c_3 - b_3c_2\right) - a_2b_2\left(b_1c_3 - b_3c_1\right) + a_3b_3\left(b_1c_2 - b_2c_1\right)}$,

$b_1 = \dfrac{1}{r_0}K_1(\beta_1 r_0) + \beta_1 K_0(\beta_1 r_0)$, $b_2 = \dfrac{1}{r_0}K_1(\beta_2 r_0) + \beta_2 K_0(\beta_2 r_0)$,

$b_3 = \dfrac{1}{r_0}K_1(\beta_3 r_0)$, $c_1 = \dfrac{1}{r_0}K_1(\beta_1 r_0)$, $c_2 = \dfrac{1}{r_0}K_1(\beta_2 r_0)$,

$c_3 = \dfrac{1}{r_0}K_1(\beta_3 r_0) + \beta_3 K_0(\beta_3 r_0)$.

饱和土体本构关系和渗流连续方程为:

$$\begin{cases} \sigma_r' = \lambda e + 2\mu\dfrac{\partial u_r}{\partial r} \\ \tau_{r\theta} = \mu\left(\dfrac{\partial u_\theta}{\partial r} + \dfrac{\partial u_r}{r\partial\theta} - \dfrac{u_\theta}{r}\right) \end{cases} \tag{34}$$

$$-\dot{P} = \alpha M\dot{e} - M\dot{\varepsilon} \tag{35}$$

式中:$\sigma_r'$、$\tau_{r\theta}$、$P$分别为有效径向应力、切应力和孔压.

式(34)、式(35)结合桩-土界面应力平衡条件,规定$q_n$作用力方向与运动方向一致为正,可得:

$$q_n = \int_0^{2\pi}\left[-\left(\sigma_r' - P\right)\cos\theta + \tau_{r\theta}\sin\theta\right]_{r=r_0}\cdot r_0\mathrm{d}\theta \tag{36}$$

将式(32)~式(35)代入式(36),经Laplace变换可得:

$$\begin{aligned}\tilde{q}_n = -\pi r_0\big[&\left(\lambda + 2\mu + \alpha M + a_1M\right)A_1\beta_1{}^2K_1\left(\beta_1 r_0\right) + \\ &\left(\lambda + 2\mu + \alpha M + a_2M\right)A_2\beta_2{}^2K_1\left(\beta_2 r_0\right) + \\ &\mu A_3\beta_3{}^2K_1\left(\beta_3 r_0\right)\big]\end{aligned} \tag{37}$$

### 3.2 桩基控制方程求解

对式(7)进行Laplace变换,得到:

$$\pi r_0\rho_p s^2\tilde{u}_p + E_pI_p\frac{\partial^4\tilde{u}_p}{\partial z^4} + \tilde{q}_n = 0 \tag{38}$$

化简整理得:

$$\frac{\partial^4\tilde{u}_p}{\partial z^4} - \frac{4\left(\tilde{q}_{nn} - r_0{}^2\rho_p s^2\right)}{r_0{}^4\cdot E_p}\tilde{u}_p = 0 \tag{39}$$

式中:$\tilde{q}_{nn} = -\tilde{q}_n/\pi\tilde{u}_p$.

求解式(39)可得桩基位移表达式:

$$\begin{aligned}\tilde{u}_p = {}&K_1\cos\left(\xi z\right) + K_2\sin\left(\xi z\right) + K_3\mathrm{ch}\left(\xi z\right) + \\ &K_4\mathrm{sh}\left(\xi z\right)\end{aligned} \tag{40}$$

结合定解条件式(14)、式(15),可推导出待定系数$K_1$、$K_2$、$K_3$、$K_4$的具体表达式.

其中,

$K_1 = K_3 = -\dfrac{2}{\pi r_0{}^4}\tilde{P}(s)\cdot\dfrac{\mathrm{ch}\left(\xi H\right)\sin\left(\xi H\right) - \mathrm{sh}\left(\xi H\right)\cos\left(\xi H\right)}{\left[1 - \mathrm{ch}\left(\xi H\right)\cos\left(\xi H\right)\right]\xi^3E_p}$,

$K_2 = -\dfrac{2}{\pi r_0{}^4}\tilde{P}(s)\cdot\dfrac{1 - \mathrm{sh}\left(\xi H\right)\sin\left(\xi H\right) - \mathrm{ch}\left(\xi H\right)\cos\left(\xi H\right)}{\left[1 - \mathrm{ch}\left(\xi H\right)\cos\left(\xi H\right)\right]\xi^3E_p}$,

$K_4 = \dfrac{2}{\pi r_0{}^4}\tilde{P}(s)\cdot\dfrac{1 + \mathrm{sh}\left(\xi H\right)\sin\left(\xi H\right) - \mathrm{ch}\left(\xi H\right)\cos\left(\xi H\right)}{\left[1 - \mathrm{ch}\left(\xi H\right)\cos\left(\xi H\right)\right]\xi^3E_p}$,

$\xi = \sqrt[4]{\dfrac{4\left(\tilde{q}_{nn} - r_0{}^2\rho_p s^2\right)}{r_0{}^4\cdot E_p}}$.

至此,桩-土系统的位移场和应力场均已确定,结合初始条件式(8)、式(9)进行Laplace反演得到相应时域解.本文采用Crump[27]构造的Laplace逆变换公式进行反演.

$$\begin{aligned}f(t) = \frac{\mathrm{e}^{ct}}{T}\Bigg\{&\frac{1}{2}\mathrm{Re}\{F(c)\} + \sum_{k=1}^{N}\Bigg[\mathrm{Re}F\left(c + \frac{k\pi\mathrm{i}}{T}\right)\cos\frac{k\pi t}{T} - \\ &\mathrm{Im}F\left(c + \frac{k\pi\mathrm{i}}{T}\right)\sin\frac{k\pi t}{T}\Bigg]\Bigg\}\end{aligned} \tag{41}$$

式中:$c$、$T$均为计算参数,且$T \geqslant t$,计算中取$T = 2t$,$c \times T = 5$;$N$为级数截取项数;i为虚数单位.试算表

明,$N$取50时,能满足精度要求.

## 4 方法验证

文献[23]给出了单相弹性土中桩基在三角形冲击荷载作用下水平振动时的桩顶位移解.取参数$\rho_f=0$、$b=0$,将本文桩侧饱和土退化到单相介质.计算参数取$H/r_0=75$,$E_p/E_s=100$,$\rho_p/\rho_s=1.6$,$v_s=0.4$.

验证结果如图2所示,本文解与文献解一致.在荷载作用期间,桩顶位移均先增大后减小;荷载作用结束后,桩顶位移先急速减小再缓慢波动到初始状态.荷载作用结束后,本文解与文献解略有差异,可能的原因如下:文献[23]中Mamoon求解控制方程时采用了分步时间积分,而本文采用Helmholtz势函数解耦方程并运用Crump构造的Laplace逆变换进行数值计算,导致计算结果在荷载作用结束后产生差异.

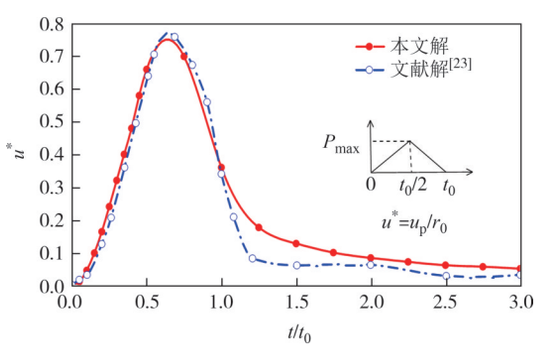



图2 与文献[23]计算结果对比图

Fig.2 Comparison of calculation results with reference [23]

## 5 算例分析

采用表1所示参数对三角形冲击荷载下的桩-土耦合振动响应进行分析.

图3给出了三角形冲击荷载作用期间桩顶位移时域响应.图4为不同桩土模量比及不同孔隙率下桩顶最大位移随渗透系数的变化规律.由图3可知,桩顶位移峰值因惯性滞后于三角形冲击荷载峰值.荷载作用时间越长,桩顶位移峰值越大.图4表明,当渗透系数$1\times10^{-5}\ \text{m/s}\leqslant k_d\leqslant1\times10^{-1}\ \text{m/s}$时,桩顶最大位移随渗透系数增加而增大,当渗透系数$k_d\geqslant1\times10^{-1}\ \text{m/s}$或渗透系数$k_d\leqslant1\times10^{-5}\ \text{m/s}$时,渗透系数变化对桩顶最大位移均无显著影响.产生这种现象的原因是渗透系数$k_d\geqslant1\times10^{-1}\ \text{m/s}$时,孔隙水处于敞开状态,能够迅速发生渗透;渗透系数$k_d\leqslant1\times10^{-5}\ \text{m/s}$时,孔隙水处于封闭状态,很难发生渗透,所以渗透系数的进一步减小也不再影响其渗透性.

**表1 算例分析计算参数**

**Tab.1 Calculation parameters analyzed by examples**

| $H$/m | $r_0$/m | $E_p$/GPa | $\rho_p$/(kg·m$^{-3}$) | $E_s$/MPa | $\rho_s$/(kg·m$^{-3}$) | $K_s$/GPa | $\rho_f$/(kg·m$^{-3}$) |
|---|---|---|---|---|---|---|---|
| 10 | 0.3 | 25.5 | 2 500 | 27 | 2 700 | 36 | 1 000 |
| $K_f$/GPa | $v_s$ | $n$ | $k_d$/(m·s$^{-1}$) | $\zeta$ | $P_{max}$/kN | $t_0$/s | $g$/(m·s$^{-2}$) |
| 2 | 0.35 | 0.375 | $1\times10^{-5}$ | 0.01 | 1 000 | 0.02 | 10 |

注:$E_s$为土体弹性模量;$K_f$为孔隙水体积模量;$v_s$为土体泊松比.

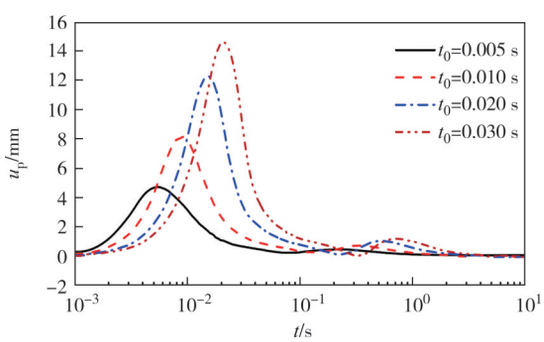



图3 桩顶位移响应

Fig.3 Pile top displacement response

由图4可以看出,孔隙率相同时,桩土模量比越大,桩顶最大位移越大;桩土模量比相同时,孔隙率越大,桩顶最大位移越大且桩顶最大位移对渗透系数变化越敏感.孔隙率从$n=0.1$增加到$n=0.4$时,桩土模量比$E_p/E_s=1\,000$时的桩顶最大位移差值约为$E_p/E_s=500$时的2倍,且倍数关系不受渗透系数影响.

图5分别给出了三角形冲击荷载作用期间,桩顶处桩-土界面有效径向应力、切应力和孔压的时域

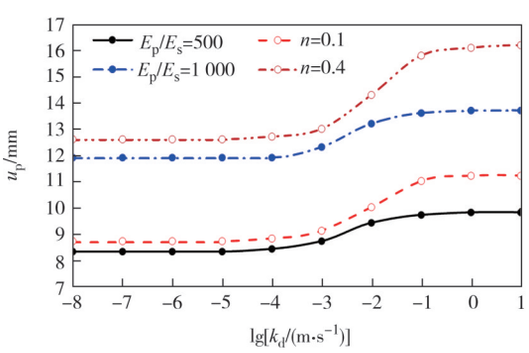
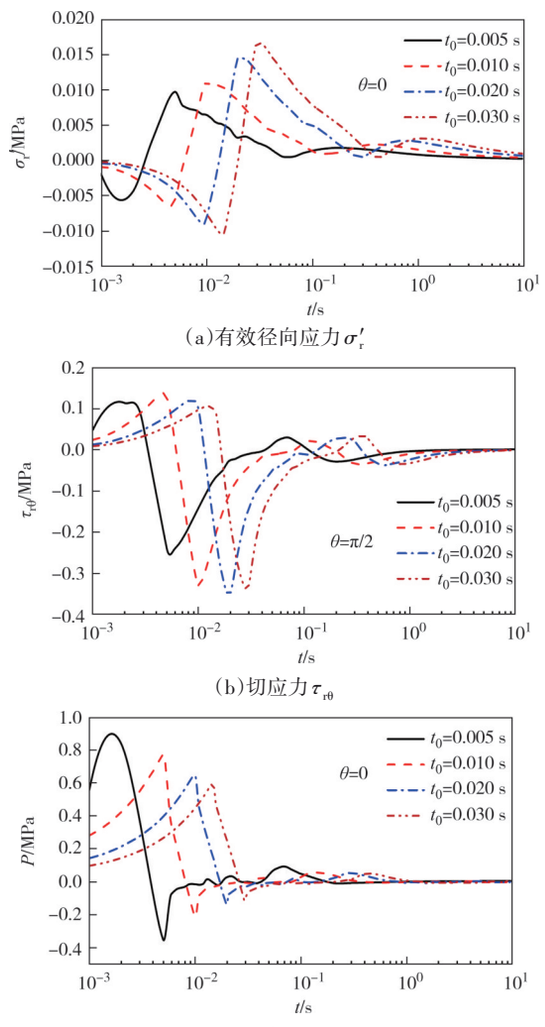



图4 渗透系数对桩顶最大位移的影响

Fig.4 Influence of permeability coefficient on maximum displacement of pile top

响应.由图可知,有效径向应力峰值随荷载作用时间增加而增大,孔压峰值则随时间增加而减小,切应力峰值变化规律与作用时间无必然联系.孔压的时域响应分析表明,荷载作用时间越短,孔压越来不及消散,故而孔隙水承担的应力越多,孔压峰值也越大.同一作用时间下,荷载达到峰值时,孔压达到桩-土耦合振动全过程峰值;荷载作用结束时,有效径向应力和切应力均达到振动全过程峰值.三角形冲击荷载作用结束后,桩-土系统逐渐恢复到初始状态.




(a)有效径向应力 $\sigma'_r$

(b)切应力 $\tau_{r\theta}$

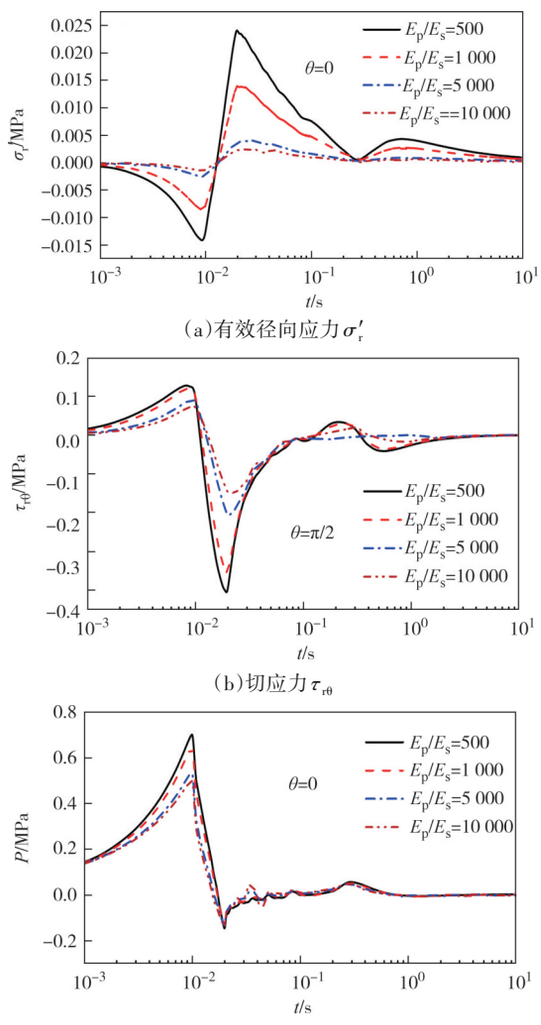
(c)孔压 $P$

图5　荷载作用时间对桩-土界面应力的影响

Fig.5　Effect of loading time on the interface stress of pile-soil

结合图3可知,由于惯性效应,桩基位移峰值点滞后于荷载峰值点.根据力平衡条件,外荷载达到峰值时,土体应力也达到峰值.因此桩基位移场反应滞后于桩周土体应力场.

图6分别给出了桩模量恒定时,不同土体模量下桩顶处桩-土界面的有效径向应力、切应力和孔压的时域响应.图6显示,桩土模量比越小,有效径向应力、切应力和孔压峰值越大且有效径向应力和切应力在荷载作用结束后波动越大,孔压波动越小.此外,桩土模量比在从500增大至5 000时,对桩-土界面应力影响显著,而从5 000增大到10 000时,桩土模量比对桩-土界面应力影响较小.




(a)有效径向应力 $\sigma'_r$

(b)切应力 $\tau_{r\theta}$

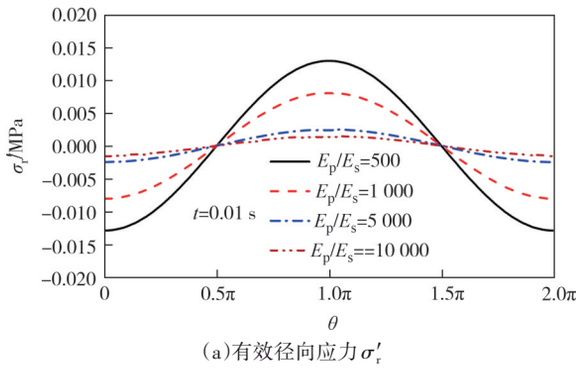
(c)孔压 $P$

图6　桩-土模量比对桩-土界面应力的影响

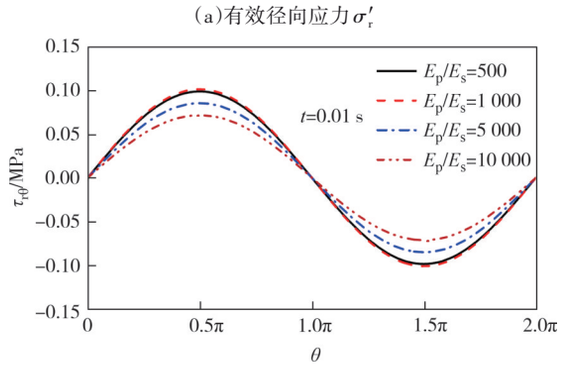
Fig.6　Effect of pile-soil modulus ratio on pile-soil interface stress

图7分别给出了在桩模量恒定,不同土体模量下桩顶处桩-土界面的有效径向应力、切应力和孔压沿桩周分布.图7显示,桩-土界面的有效径向应力和孔压沿桩周(0~2π)呈余弦分布,$\theta=0$和$\theta=\pi$处达到峰值;切应力呈正弦分布,$\theta=\pi/2$和$\theta=3\pi/2$处达到峰值.

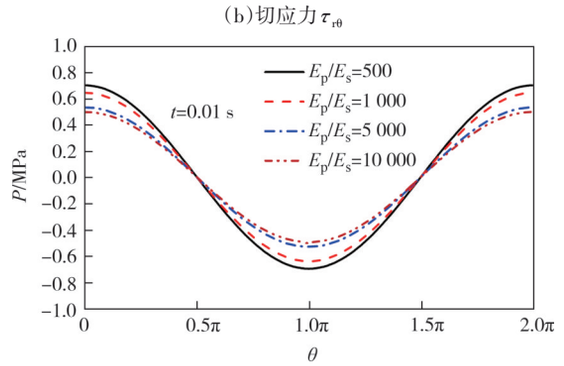
图8分别给出了土体不同渗透系数下桩-土界面处有效径向应力、切应力和孔压的时域响应.图8显示,渗透系数越小,有效径向应力峰值越小,孔压




(a)有效径向应力 $\sigma'_r$



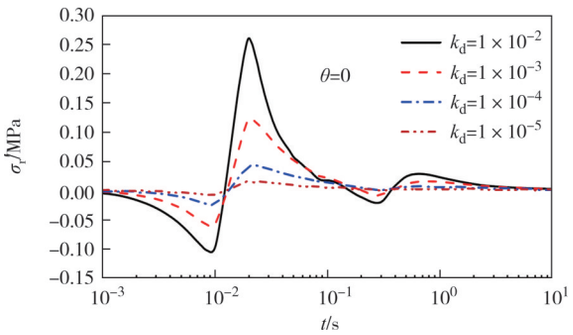

(b)切应力 $\tau_{r\theta}$



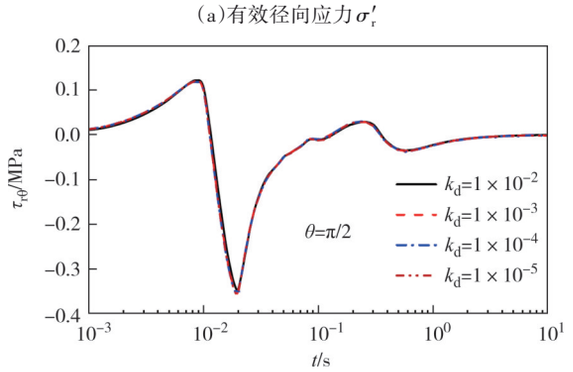

(c)孔压 $P$

图 7 桩-土界面应力沿桩周分布

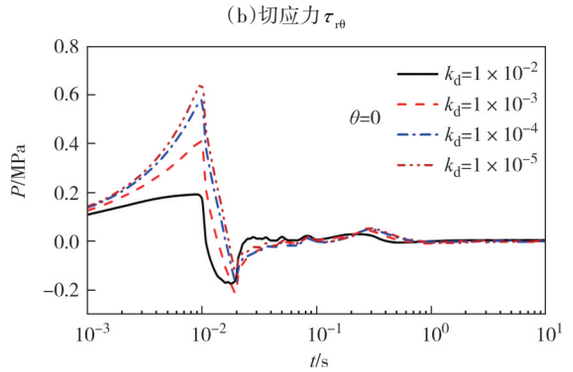
Fig.7 Distribution of pile-soil interface stress around the pile




(a)有效径向应力 $\sigma'_r$




(b)切应力 $\tau_{r\theta}$




(c)孔压 $P$

图 8 渗透系数对桩-土界面应力的影响

Fig.8 Effect of permeability coefficient on pile-soil interface stress

峰值越大,而切应力几乎不受土体渗透系数变化的影响.在渗透系数 $k_d$ 从 $1\times10^{-2}$ m/s 减小到 $1\times10^{-4}$ m/s 时,有效径向应力和孔压变化显著,从 $1\times10^{-4}$ m/s 减小到 $1\times10^{-5}$ m/s 时变化不明显,即渗透系数小于 $1\times10^{-4}$ m/s 时,桩-土界面处的有效径向应力和孔压趋于稳定,随渗透系数变化的幅度减小.

图 9 和图 10 给出了桩顶水平面处孔压在桩周土中的分布.由图可知,不同渗透系数的最大孔压均出现在桩-土界面处,但孔压最大值和桩周土中孔压分布均与渗透系数有关.当渗透系数较大时,最大孔压较小且孔压分布较分散;当渗透系数较小时,最大孔压较大且孔压主要集中在桩周.图 11 和图 12 给出了桩顶水平面处有效径向应力在桩周土中的分布.图 11 显示,不同渗透系数下,最大有效径向应力均出现在桩周土中.

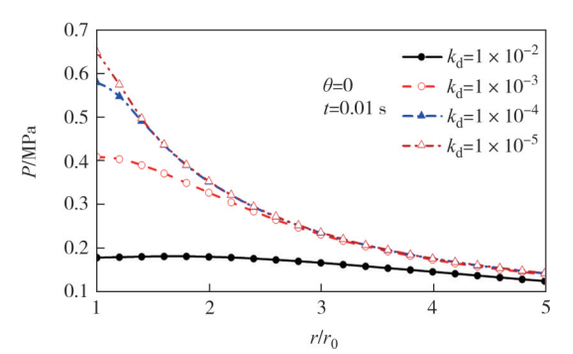
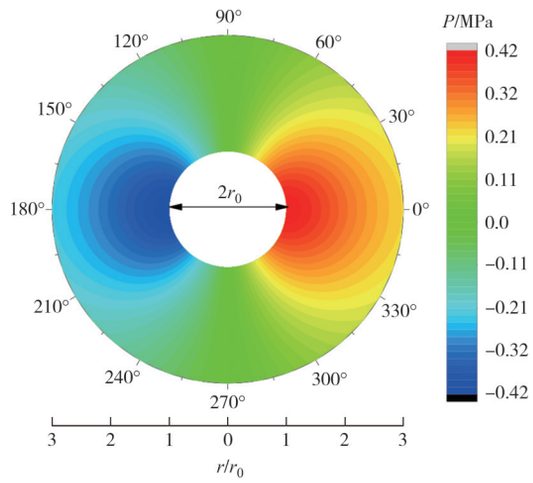


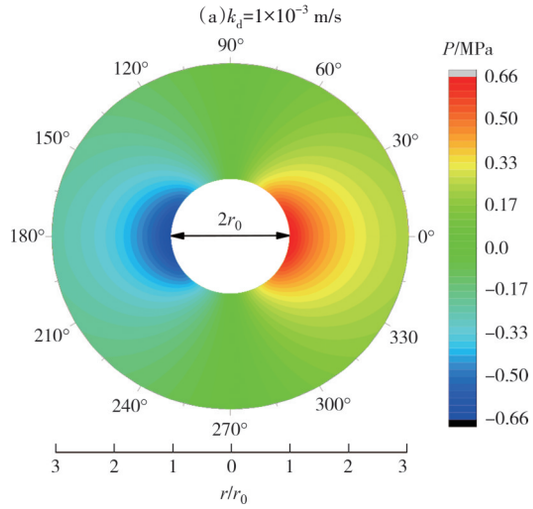

图 9 孔压沿径向分布

Fig.9 Radial distribution of pore pressure

由图 9~图 12 可知:在三角形冲击荷载作用下,由于荷载快速增加,孔隙水来不及渗透,导致桩-土界面孔隙水压力迅速增大.当渗透系数越小,孔隙




(a)$k_d$=1×10$^{-3}$ m/s




(b)$k_d$=1×10$^{-5}$ m/s

图 10　桩周土中孔压水平面分布($t$ = 0.01 s)

Fig.10　Horizontal distribution of pore pressure in soil around pile

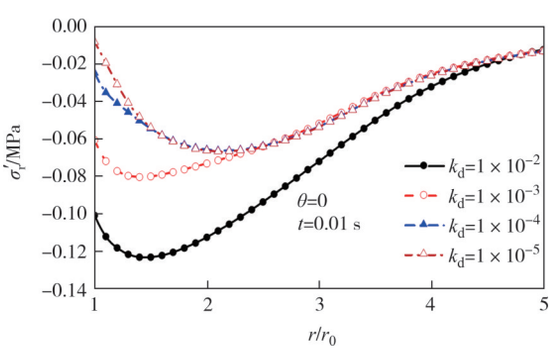
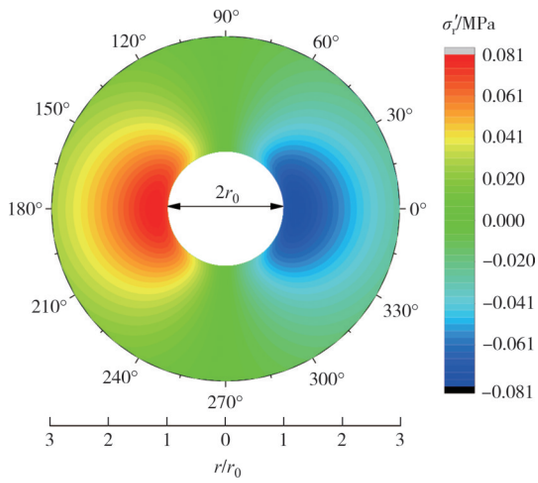


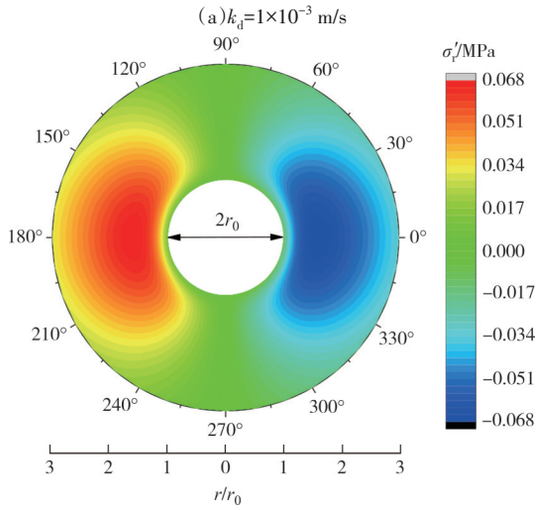

图 11　有效径向应力沿径向分布

Fig.11　Radial distribution effective radial stress

水渗透越困难,导致桩–土界面土体孔隙水压力越难以消散,桩–土界面土体应力主要由孔隙水压力承担,因此桩–土界面处土体的有效径向应力越小.同时,渗透系数越小,距离桩–土界面较远处的饱和土体孔压越小,从而使得最大有效径向应力出现在较远处.




(a)$k_d$=1×10$^{-3}$ m/s




(b)$k_d$=1×10$^{-5}$ m/s

图 12　桩周土中有效径向应力水平面分布 ($t$ = 0.01 s)

Fig.12　Horizontal distribution of effective radial stress in soil around pile

## 6　结 论

本文采用Euler梁建立桩–饱和土耦合振动的平面应变简化模型,研究三角形水平冲击荷载下桩顶位移、桩–土界面及桩周土的动力响应,得出以下结论:

1)三角形冲击荷载作用时间越长,桩顶位移响应越大,桩周土体有效径向应力峰值越大而孔压峰值越小;相同荷载时间下,桩基位移场反应因惯性效应滞后于桩周土体的应力场.

2)当桩周饱和土渗透系数 $k_d \leqslant 1 \times 10^{-5}$ m/s 时,孔隙水呈封闭状态;而渗透系数 $k_d \geqslant 1 \times 10^{-1}$ m/s 时,孔隙水处于敞开状态;这两种情况下,渗透系数变化对桩顶位移不会产生明显影响.当渗透系数 $1 \times 10^{-5}$ m/s $\leqslant k_d \leqslant 1 \times 10^{-1}$ m/s 时,孔隙率越大,渗透系数对桩顶位移影响越显著.

3)桩周饱和土渗透系数不仅影响桩周土体孔压

和有效径向应力大小,而且会改变孔压和有效径向应力分布.在渗透系数较小的饱和土体中,可以通过增大桩径和桩基模量的方式来增大桩基刚度,避免桩周土体液化导致桩基失稳.

## 参考文献


[1] NOGAMI T, KONAGAI K. Time domain axial response of dynamically loaded single piles [J]. Journal of Engineering Mechanics, 1986, 112(11): 1241-1252.

[2] NOGAMI T, KONAGAI K. Time domain flexural response of dynamically loaded single piles [J]. Journal of Engineering Mechanics,1988,114(9):1512-1525.

[3] NOVAK M. Dynamic stiffness and damping of piles [J]. Canadian Geotechnical Journal,1974,11(4):574-598.

[4] NOVAK M, NOGAMI T. Soil-pile interaction in horizontal vibration [J]. Earthquake Engineering & Structural Dynamics, 1977,5(3):263-281.

[5] NOVAK M, ABOUL-ELLA F. Impedance functions of piles in layered media [J]. Journal of the Engineering Mechanics Division,1978,104(3):643-661.

[6] NOVAK M, ABOUL-ELLA F, NOGAMI T. Dynamic soil reactions for plane strain case [J]. Journal of the Engineering Mechanics Division,1978,104(4):953-959.

[7] GAZETAS G, DOBRY R. Horizontal response of piles in layered soils [J]. Journal of Geotechnical Engineering, 1984, 110(1): 20-40.

[8] 尚守平,余俊,王海东,等. 饱和土中桩水平振动分析[J].岩土工程学报, 2007, 29(11): 1696-1702.
SHANG S P, YU J, WANG H D, et al. Horizontal vibration of piles in saturated soil [J]. Chinese Journal of Geotechnical Engineering, 2007, 29(11): 1696-1702.(in Chinese)

[9] 余俊, 尚守平,李忠,等. 饱和土中端承桩水平振动动力响应分析[J]. 岩土工程学报,2009,31(3):408-415.
YU J, SHANG S P, LI Z, et al. Dynamical characteristics of an end bearing pile embedded in saturated soil under horizontal vibration[J]. Chinese Journal of Geotechnical Engineering, 2009, 31(3): 408-415.(in Chinese)

[10] 余俊,尚守平,李忠,等. 饱和土中桩水平振动引起土层复阻抗分析研究[J]. 岩土力学, 2009, 30(12): 3858-3864.
YU J, SHANG S P, LI Z, et al. Study of resistance factor of saturated soil caused by horizontal vibration of pile[J]. Rock and Soil Mechanics, 2009, 30(12): 3858-3864.(in Chinese)

[11] 余俊,尚守平,黄娟,等. Biot动力固结方程简化模型在桩水平动力响应中适用性研究[J]. 岩土工程学报,2014,36(8): 1558-1563.
YU J, SHANG S P, HUANG J, et al. Applicability of simplified model of Biot's dynamic consolidation equation to response of horizontal vibration of piles[J]. Chinese Journal of Geotechnical Engineering,2014,36(8):1558-1563.(in Chinese)

[12] 刘林超,闫启方,闫盼. 考虑三维波动的饱和土中管桩群桩的水平振动研究[J]. 岩土力学,2017,38(10):2817-2825.
LIU L C, YAN Q F, YAN P. Horizontal vibration of pipe pile groups in saturated soil considering three-dimensional wave effects[J]. Rock and Soil Mechanics,2017,38(10):2817-2825.(in Chinese)

[13] HU A F, FU P, XIA C Q, et al. Lateral dynamic response of a partially embedded pile subjected to combined loads in saturated soil[J]. Marine Georesources & Geotechnology, 2017, 35(6): 788-798.

[14] 赵密, 黄义铭, 王丕光, 等. 桩顶水平动荷载作用下水-桩-土相互作用的解析解[J]. 岩土工程学报, 2022,44(5): 907-915.
ZHAO M, HUANG Y M, WANG P G, et al. Analytical solution for water-pile-soil interaction under horizontal dynamic loads on pile head [J]. Chinese Journal of Geotechnical Engineering, 2022,44(5):907-915.(in Chinese)

[15] 范小雪,李原,吴文兵,等. 饱和土中大直径缺陷桩水平振动响应研究[J]. 岩石力学与工程学报,2020,39(2):413-423.
FAN X X, LI Y, WU W B, et al. Horizontal vibration response of defective large-diameter piles embedded in saturated soils [J]. Chinese Journal of Rock Mechanics and Engineering, 2020, 39(2): 413-423.(in Chinese)

[16] 郑长杰, 刘汉龙, 丁选明, 等. 饱和黏性土地基中现浇大直径管桩水平振动响应解析解[J]. 岩土工程学报, 2014, 36(8): 1447-1454.
ZHENG C J, LIU H L, DING X M, et al. Analytical solution of horizontal vibration of cast-in-place large-diameter pipe piles in saturated soils[J]. Chinese Journal of Geotechnical Engineering, 2014, 36(8): 1447-1454.(in Chinese)

[17] 郑长杰,丁选明,栾鲁宝. 黏弹性地基中管桩水平动力特性分析[J]. 岩土力学, 2017, 38(1): 26-32.
ZHENG C J, DING X M, LUAN L B. Analysis of lateral dynamic response of pipe pile in viscoelastic soil layer[J]. Rock and Soil Mechanics, 2017, 38(1): 26-32.(in Chinese)

[18] HU A F, FU P, XIA C Q, et al. Horizontal impedances of saturated soil layer with radially inhomogeneous boundary zone[J]. Soil Dynamics and Earthquake Engineering, 2018, 111: 184-192.

[19] ZHENG C J, LUAN L B, QIN H Y, et al. Horizontal dynamic response of a combined loaded large-diameter pipe pile simulated by the Timoshenko beam theory [J]. International Journal of Structural Stability and Dynamics, 2020, 20(2): 2071003.

[20] 章敏, 王星华, 冯国瑞. 非饱和土中端承桩水平振动特性研究[J]. 岩土力学,2015,36(2):409-422.
ZHANG M, WANG X H, FENG G R. Horizontal vibration of an end-bearing pile in unsaturated soil [J]. Rock and Soil Mechanics, 2015, 36(2): 409-422.(in Chinese)

[21] 郭诚. SH波作用下非饱和土中管桩水平动力特性的理论及试验研究[D]. 太原: 太原理工大学, 2018: 27-28.
GUO C. Theoretical and experimental study on horizontal dynamic characteristics of pipe pile in unsaturated soil under SH wave[D]. Taiyuan: Taiyuan University of Technology, 2018: 27-28 (in Chinese).

[22] 杨紫健, 吴文兵, 张云鹏, 等. 考虑竖向荷载影响的非饱和地基中桩的水平振动[J]. 岩石力学与工程学报, 2022, 41(增刊1): 2979-2990.
YANG Z J, WU W B, ZHANG Y P, et al. Horizontal vibration of piles in unsaturated foundation considering vertical load [J]. Chinese Journal of Rock Mechanics and Engineering, 2022, 41(Sup.1): 2979-2990.(in Chinese)

[23] MAMOON S M, BANERJEE P K. Time-domain analysis of dynamically loaded single piles [J]. Journal of Engineering Mechanics, 1992, 118(1): 140-160.

[24] 刘圆圆, 王星华, 章敏, 等. 饱和土中单桩水平瞬态响应研究[J]. 岩土力学, 2013, 34(9): 2699-2706.
LIU Y Y, WANG X H, ZHANG M, et al. Transient response of single pile under horizontal load in saturated soil[J]. Rock and Soil Mechanics, 2013, 34(9): 2699-2706.(in Chinese)

[25] 尚微. 饱和土中管桩水平瞬态动力特性研究[D]. 太原: 太原理工大学, 2018.
SHANG W. Study on horizontal transient dynamic characteristics of pipe pile in saturated soil[D]. Taiyuan: Taiyuan University of Technology, 2018.(in Chinese)

[26] 赵仓龙,章敏,李亚楠,等. 层状饱和土中管桩瞬态扭转振动研究[J]. 应用力学学报, 2022, 39(3): 516-526.
ZHAO C L, ZHANG M, LI Y N, et al. Transient torsional response of a pipe pile embedded in layered saturated soil [J]. Chinese Journal of Applied Mechanics, 2022, 39(3): 516-526.(in Chinese)

[27] CRUMP K S. Numerical inversion of Laplace transforms using a Fourier series approximation [J]. Journal of the ACM, 1976, 23(1):89-96.